Geochemical Journal, Vol. 47, pp. 201 to 217, 2013

Petrological vestiges of the Late Jurassic–Early Cretaceous transition from rift to back-arc basin in southernmost Chile: New age and geochemical data from the Capitán Aracena, Carlos III, and Tortuga ophiolitic complexes

M. CALDERÓN,[1]* C. F. PRADES,[1] F. HERVÉ,[1,2] V. AVENDAÑO,[1] C. M. FANNING,[3] H.-J. MASSONNE,[4] T. THEYE[4] and A. SIMONETTI[5]

[1]Departamento de Geología, Facultad de Ciencias Físicas y Matemáticas, Universidad de Chile, Casilla 13518, Correo 21, Santiago, Chile
[2]Escuela de Ciencias de la Tierra, Universidad Andrés Bello, Salvador Sanfuentes 2375, Santiago, Chile
[3]Research School of Earth Sciences, The Australian National University, Canberra, ACT. 0200, Australia
[4]Institut für Mineralogie und Kristallchemie, Universität Stuttgart, Azenbergstrasse 18, D-70174, Stuttgart, Germany
[5]Department of Earth and Atmospheric Sciences, University of Alberta, 1-26 Earth Sciences Building, Edmonton, Alberta, Canada T6G 2E3

(*Received January 27, 2012; Accepted November 9, 2012*)

The ophiolitic remnants of the Upper Mesozoic Rocas Verdes basin in southernmost South America were studied from the perspectives of petrography, chemistry of minerals, bulk-rock geochemistry, and U–Pb geochronology. The study aimed to unravel the tectonic, magmatic, and metamorphic evolution of a suprasubduction rift zone that underwent a transition to a back-arc basin. The rifting phase and bimodal magmatism within the Rocas Verdes basin started prior to or during the Late Jurassic, as indicated by a gabbro in contact with pillow basalts that dated at 154 Ma. In the Late Jurassic Capitán Aracena and Carlos III complexes, tholeiitic basalts are geochemically comparable to enriched mid-oceanic ridge basalts. Back-arc basin development continued for 35 myr until the Early Cretaceous, as suggested by the ages of detrital zircons in cherty layers within pillow basalts and metamorphic titanite that crystallized during seafloor metamorphism near the spreading/magmatic axis. In the Early Cretaceous Tortuga Complex, tholeiitic basalts are comparable to normal mid-oceanic ridge basalts. Non-deformative metamorphism converted the primary mineralogy of the ophiolites to low- to intermediate-grade metamorphic assemblages formed during ocean-floor type alteration in a suprasubduction setting. Fossilized bacteria, preserved as rounded aggregates of titanite microcrystals, were identified in the pillow basalts up to the Early Cretaceous. The Rocas Verdes basin closed during the Andean orogeny, which started during the Late Cretaceous, and ophiolites were tectonically juxtaposed and thrust over the sedimentary infill of the quasi-oceanic basin in which they developed. The tectonic emplacement of the ophiolitic complexes was complete before the latest Cretaceous, as indicated by crystallization ages of granites intruded into the ophiolitic complexes.

Keywords: Rocas Verdes ophiolites, rift to back-arc basin transition, U–Pb dating, geochemistry, mineral chemistry, microbes

INTRODUCTION

Ophiolite complexes, the igneous constituents of idealized oceanic crust and upper lithospheric mantle, consist of metamorphosed basaltic lava flows grading downward to the level of sheeted dike complexes, massive diabase and gabbroic units, and ultimately ultramafic rocks at the base (Penrose-type ophiolite; Anonymous, 1972). Initially interpreted as allochthonous oceanic fragments formed at mid-oceanic ridges, most documented ophiolites display distinctive lithological associations, architecture, and geochemistry that have been attributed to tectonomagmatic evolution in fore-arc, embryonic arc, or back-arc regions of suprasubduction zone environments (cf., Miyashiro, 1973; Pearce *et al*., 1984; Stern and de Wit, 2003; Dilek and Furnes, 2011). Suprasubduction zone ophiolites are constituents of most Phanerozoic orogenic belts, indicating that oceanic-type crust has been generated in subduction rollback cycles and tectonically emplaced over continental rocks through collisional/accretionary processes (Dalziel, 1986; Dilek, 2003).

It is noteworthy that ophiolites include fossil and subaerial remnants of seafloor spreading systems and bear record of the earliest documented forms of microbial life in the Earth (Furnes *et al*., 2004). The interaction of hydrothermal fluids with basaltic rocks at temperatures below *ca*. 113°C (Stetter, 2006) allows extremophile microorganisms (Thorseth *et al*., 2001) that obtain energy

*Corresponding author (e-mail: mccaldera@gmail.com)

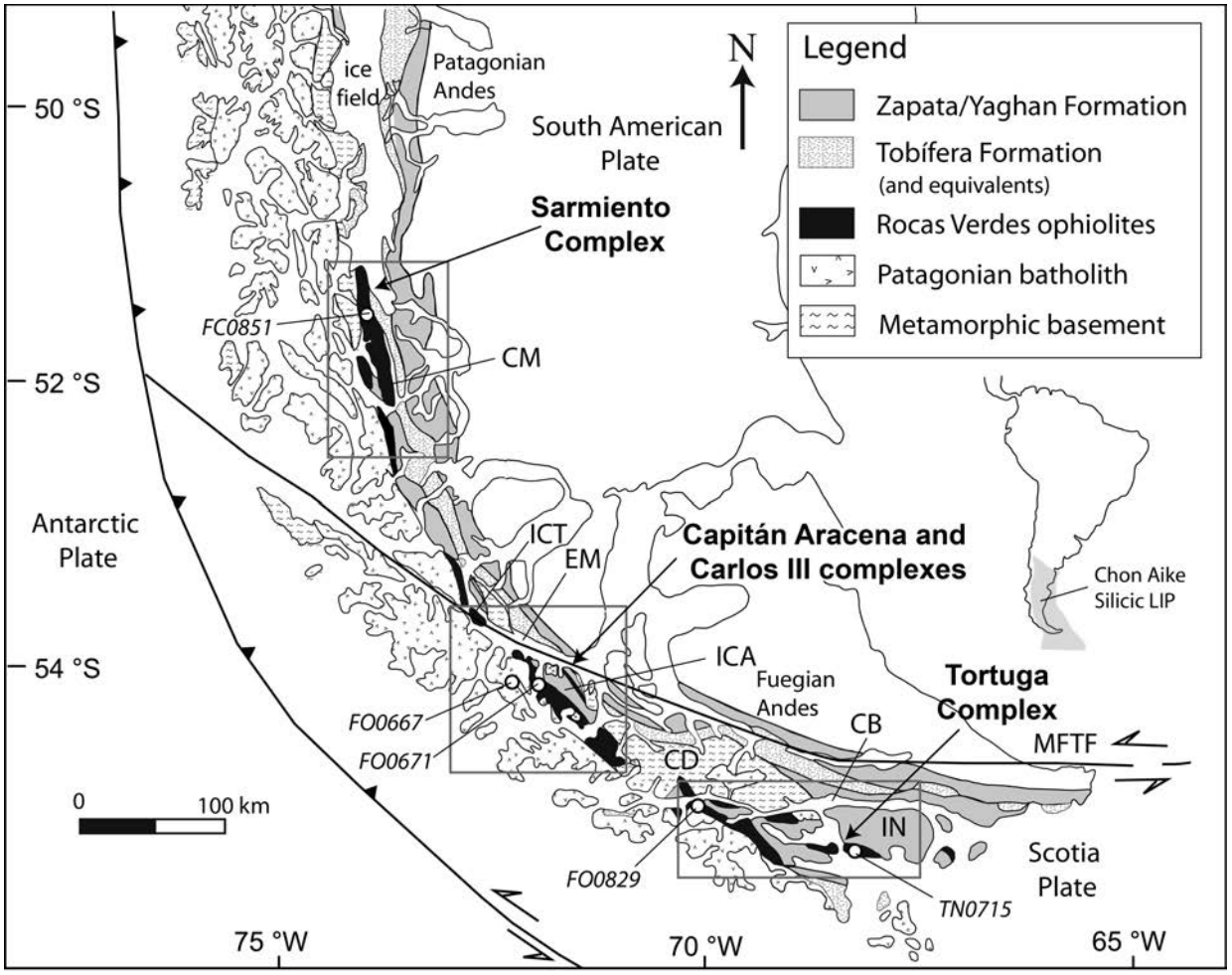

Fig. 1. A geological sketch map showing the distribution of ophiolitic rocks in the archipelagos of southernmost Chile. The location of the Chon Aike silicic large igneous province (LIP) is also indicated. Abbreviations—CM, Canal de las Montañas; CB, Canal Beagle; EM, Estrecho de Magallanes; ICT, Isla Carlos III; ICA, Isla Capitán Aracena; IN, Isla Navarino; MFTF, Magallanes Fagnano transform fault. For the names of other places, please refer to the corresponding references. Locations of samples dated by U–Pb methods are highlighted.

by catalyzing reduction-oxidation reactions in disequilibrium with the seawater environment to colonize seafloor extrusive volcanic rocks.

The Jurassic to Early Cretaceous Rocas Verdes basin (Katz, 1964; Dalziel *et al.*, 1974; Dalziel, 1981; Stern and deWit, 2003; Calderón *et al.*, 2007a) is represented by discontinuous exposures of ophiolitic complexes along the southernmost Andes of South America (Fig. 1). The Rocas Verdes basin is globally associated with a major ophiolite pulse and coeval with the emplacement of the Jurassic Chon Aike silicic large igneous province and the early break-up of Gondwana in eastern Patagonia (Fig. 1; Bruhn *et al.*, 1978; Dalziel *et al.*, 2000; Pankhurst *et al.*, 2000; Vaughan and Scarrow, 2003). The Rocas Verdes ophiolites (nomenclature of Stern and de Wit, 2003) host critical information about back-arc basin evolution at the southwestern convergent margin of South America, which has a reconstructed basin configuration analogous to the present-day Sea of Japan marginal basin (as suggested by Dalziel *et al.*, 1974; Wilson, 1991; Fildani and Hessler, 2005; Romans *et al.*, 2010) and/or the Gulf of California (Alabaster and Storey, 1990). The Rocas Verdes ophiolites are particularly well suited for examining the petrological transition from rift to back-arc basin that preceded the mid- to Late Cretaceous basin closure and orogenesis in the Patagonian Andes (Dalziel, 1981; Cunningham, 1994; Fildani *et al.*, 2003; Klepeis *et al.*, 2010; Calderón *et al.*, 2012).

To date, geochemical and isotopic studies of the Rocas Verdes ophiolites have focused mainly on the Sarmiento and Tortuga complexes (Saunders *et al.*, 1979; Stern, 1979, 1980, 1991; Fildani and Hessler, 2005; Calderón *et*

al., 2007a, b) that represent rifting and back-arc basin stages, respectively. This paper presents new petrological, geochemical, and geochronological data for ophiolitic rocks of the less-studied Capitán Aracena and Carlos III complexes and discusses their significance for the geodynamic evolution of the southernmost margin of South America. U–Pb dating of zircon and titanite provides a precise time frame of magmatic and metamorphic processes through the evolution of the basin. Additionally, structures similar to microbial fossils in Early Cretaceous mid-ocean-ridge-type basalts from the Tortuga ophiolite are reported for the first time.

Geological Background

The Rocas Verdes ophiolites are tectonically incorporated into the Andes of southern South America and the island of South Georgia (51°–55°S) and preserve an incomplete (lacking ultramafic rocks) ophiolite pseudostratigraphy. They have been interpreted as the igneous remnants of the Late Jurassic to Early Cretaceous Rocas Verdes back-arc basin that developed along the southwestern convergent margin of Gondwana (Katz, 1964; Dalziel *et al*., 1974; Mukasa and Dalziel, 1996; Stern and de Witt, 2003; Calderón *et al*., 2007a). Mafic magmatism within the Rocas Verdes basin was accompanied, in neighboring areas, by voluminous ignimbrite volcanism of the Tobifera Formation, which consists in part of basal breccias and conglomerates interpreted as syn-rift clastic deposits; these deposits unconformably overlie the Paleozoic metamorphic complexes (Bruhn *et al*., 1978; Allen, 1982; Pankhurst *et al*., 2000; Calderón *et al*., 2007a). Although the depositional contact between the Rocas Verdes ophiolites and the overlying hemipelagic sedimentary successions (Zapata and Yaghan formations) is mostly obscured by subsequent thrust-fold deformation and intrusion of plutons, exceptional outcrops exist where it is preserved (Allen, 1982; Suárez *et al*., 1985; Fildani and Hessler, 2005; Calderón, 2006). Thus, the age of the ophiolites is indirectly constrained as Tithonian to Valanginian (*ca*. 150–134 Ma) by biofacies associations in the overlying sedimentary successions (Fuenzalida and Covacevich, 1988; Suárez *et al*., 1985). The ophiolites underwent seafloor-type hydrothermal metamorphism (Stern *et al*., 1976; Elthon and Stern, 1978) and were subsequently buried and obducted onto the margin of South America during the ensuing phases of Andean orogenesis in the mid-Cretaceous (Katz and Watters, 1966; Dott *et al*., 1977; Dalziel, 1981; Cunningham, 1994; Fildani *et al*., 2003; Fosdick *et al*., 2011; Calderón *et al*., 2012). Granitoids consisting of hornblende–biotite tonalite, granodiorite, and restricted monzonite and monzodiorite (Katz and Watters, 1966; Godoy, 1978; Allen, 1982) intruding the ophiolite complexes are of earliest Late Cretaceous age (Hervé *et al*., 1984, 2007a; Cunningham, 1994; Calderón *et al*., 2012).

Methods

Chemical compositions of minerals were obtained from selected rock samples using a CAMECA SX100 electron microprobe (EMP) with five wavelength-dispersive spectrometers at Universität Stuttgart, Germany. Operating conditions were an acceleration voltage of 15 kV, a beam current of 15 nA, a beam size of 7–10 μm or a focused beam (for very small crystals), and 20 s counting time on the peak and on the background for each element. The standards used were natural wollastonite (Si, Ca), natural orthoclase (K), natural albite (Na), natural rhodonite (Mn), synthetic Cr_2O_3 (Cr), synthetic TiO_2 (Ti), natural hematite (Fe), natural barite (Ba), synthetic MgO (Mg), synthetic Al_2O_3 (Al), and synthetic NiO (Ni). The PaP correction procedure of CAMECA was applied. Representative data are reported in Supplementary Table S1.

Bulk-rock compositions of major and trace elements were measured with an optical ICP spectrometer at Universidad de Chile. The Th, Ta, Nb, and Hf concentrations of specific samples were determined using an ICP-MS at Servicio Nacional de Geología y Minería in Chile. The data are listed in Supplementary Table S2.

U–Pb dating was performed on zircons separated from plutonic rocks and from a cherty rock and titanite grains in polished sections using a SHRIMP. After grinding the rock, zircons were recovered using a Wilfley table and by subsequent magnetic and heavy liquid separation at Universidad de Chile. The zircons were then mounted in epoxy and polished to about half their respective thicknesses at The Australian National University. Cathodoluminescence (CL) images were obtained for every sample. SHRIMP U–Th–Pb analyses were then conducted following the procedures described in Williams (1998). The data were processed using the SQUID Excel macro of Ludwig (2000) (Supplementary Table S3). Uncertainties are reported at the 1σ level. Corrections for common Pb were made using the measured $^{238}U/^{206}Pb$ and $^{207}Pb/^{206}Pb$ ratios following Tera and Wasserburg (1972) as outlined in Williams (1998). Titanite grains on a polished section were similarly dated by U–Pb in the same laboratory (Supplementary Table S4a). The geological time scale used is that of the IUGS-ICS (http://www.stratigraphy.org).

U–Pb dating of titanite was also performed using a Nu Plasma MC-ICP-MS (Nu Instruments, Wrexham, North Wales, UK) coupled to a UP213 laser ablation system (New Wave Research, Portland, Oregon, USA) at the University of Alberta (Supplementary Table S4b). Details of the analytical protocols employed, which include external calibration, monitoring of laser-induced elemental

fractionation, and data reduction were described by Simonetti *et al*. (2006).

Petrography of the Ophiolitic Complexes

During the period 2002–2010, the authors visited ophiolite localities of the Sarmiento and Tortuga complexes and those of the less-studied Capitán Aracena and Carlos III ophiolitic complexes (Prades, 2008). The ophiolite pseudostratigraphy, as described in earlier studies (Godoy, 1978; Stern and de Wit, 2003), was recognized, sampled in the field, and complemented with petrographic data, EMP mineral compositional data, and whole-rock geochemistry.

Sarmiento Complex

The Sarmiento Complex occurs in a north–south-trending 10–20-km-wide belt bound by the South Patagonian batholith in the west and the Canal de las Montañas shear zone in the east (Fig. 1). It preserves an incomplete ophiolite pseudostratigraphy, lacking the ultramafic component. Calderón (2006) distinguished three main lithological layers: (1) a thick mafic extrusive layer of pillow basalts and breccias with intercalations of radiolarian chert; (2) a mafic–felsic extrusive layer consisting predominantly of layers of pillow basalts, including intercalations of rhyolitic tuffs, hyaloclastites, and rhyolitic and dacitic dikes, which is in turn cut by mafic intrusive bodies; and (3) a mafic–felsic intrusive layer consisting mainly of medium-grained granophyre cut by fine-grained gabbro and late subhorizontal plagiogranite dikes. The base of this unit is composed of metagabbro and amphibolite. These rocks are exposed in two north–south trending steeply dipping thrust sheets located in the central and western portions of the Sarmiento Cordillera (Rapalini *et al*., 2008; Calderón *et al*., 2012). The rocks are foliated and metamorphosed in a discontinuous way; parts of the rocks preserve original textures and structures.

Capitán Aracena Complex

To the south of and in the middle of the main trace of the Magallanes–Fagnano strike-slip fault, the Capitán Aracena Complex crops out in a northwest–southeast-trending 20-km-wide belt located to the northeast of Cordillera Darwin (Fig. 1). The mafic rocks of the ophiolite complex on Isla Capitán Aracena were mapped by Otzen (1987). They form a body elongated in a southeast–northwest direction that is thrust northward over metasedimentary rocks of the Yaghan Formation. The rocks are associated with diverse granitoid bodies that intrude them and with rhyolitic rocks of the Tobífera Formation that have field relationships that could not be established in detail during fieldwork, but that in the Sarmiento ophiolite are interbedded with the mafic rocks (Calderón *et al*., 2007b).

In at least five visited locations on Isla Capitán Aracena, basaltic pillow lavas with a maximum pillow diameter between 30 and 100 cm were observed, which are occasionally cut by mafic dikes. Bedding attitudes vary from subhorizontal to subvertical. There are also short tracts of green aphanitic foliated rocks, which despite their occasional intense foliation appear in the field to be mafic dike complexes. Coarse-grained gabbros were observed at several localities and, at some of these, were close to pillow basalts with no apparent discontinuity between them. The foliation strikes N68°–85°W with dips of 49–56°S. Even though this foliation predominates in some outcrops, it is not penetrative, and areas with strongly foliated rocks alternate with areas of unfoliated or slightly foliated rocks.

When viewed through a microscope, the mafic rocks show variable degrees of obliteration of the original texture. Primary variolitic, amygdaloidal, porphyritic, and glomerophyric textures were observed in pillow lavas, and seriate, intersertal, microgranular, and ophitic textures were observed in the dikes. In rocks having obliterated primary textures, nematoblastic, lepidoblastic, and nematolepidoblastic arrangements of neoformed minerals were observed. The primary minerals, represented only by rare relict pyroxene, are almost completely replaced by secondary minerals. The secondary minerals in the amygdaloidal pillow basalts include albite, chlorite, quartz, epidote, prehnite, rare pumpellyite, and calcite in rocks from the southeastern sector of the island; whereas these include albite, amphibole, epidote, quartz, biotite, traces of chlorite, titanite, and clinozoisite in Seno Mónica (Fig. 2). Stilpnomelane is restricted to foliated metabasalts. Pyrite and occasional chalcopyrite are also present.

Mineral chemistry Microprobe data for the pillow basalt FO0626 from Isla Capitán Aracena indicate the presence of plagioclase, epidote, and amphibole. Selected mineral analyses are listed in Table S1. The plagioclase is almost pure albite ($An_{0.6–2.0}Ab_{97.7–99.2}Or_{0.2}$). The epidote contains 11.3 to 12.6 wt% Fe_2O_3 with $XFe^{3+} = (Fe^{3+}/(Fe^{3+} + Al^{tot}))$ values between 0.22 and 0.25. The amphibole is magnesiohornblende and ferrohornblende according to the Leake *et al*. (1997) diagram.

Carlos III Complex

At the four visited locations on Isla Carlos III, pillow lavas with amygdales (some having spherulitic textures) were observed as massive green-colored rocks intruded by dikes. Foliated black shales were intercalated with the volcanic rocks. The development of secondary minerals did not obliterate the original igneous textures of these rocks and no foliation is present; consequently,

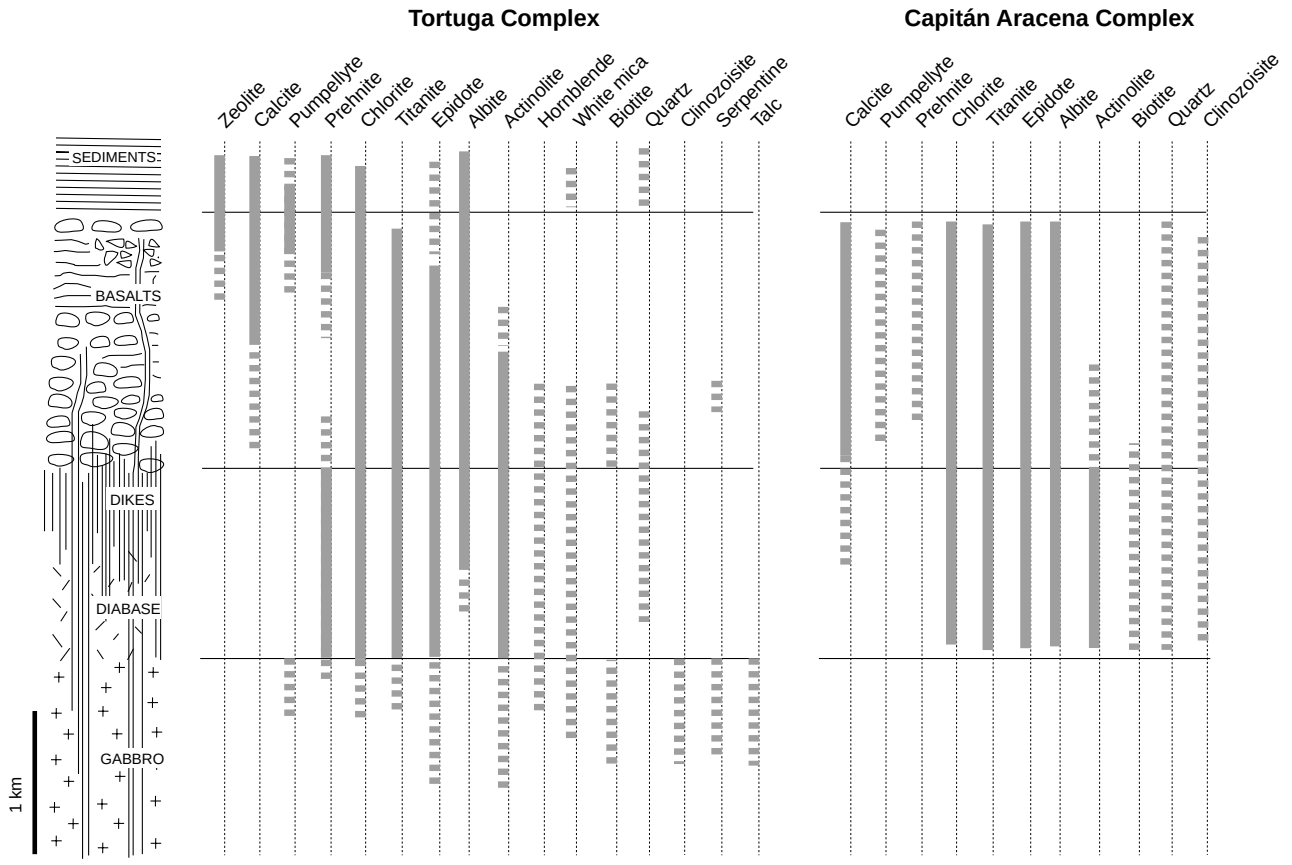

Fig. 2. Distribution of metamorphic minerals in the Tortuga and Capitán Aracena ophiolitic complexes. Pseudostratigraphy is indicated on the left-hand coordinate.

porphyritic, intersertal, amygdaloidal, spherulitic, glomerophyric, and subophitic textures were recognized. The relict primary minerals are plagioclase and clinopyroxene. The secondary minerals are albite, amphibole, chlorite, quartz, epidote, titanite, occasional clinozoisite, andradite-rich garnet, and pumpellyite (Fig. 2). Pyrite and chalcopyrite are also present.

Mineral chemistry Primary (pyroxene and plagioclase) and secondary minerals were analyzed in samples FO0335B, FO0335C, and FO0335D by EMP. A selection of the mineral analyses is listed in Table S1.

Andesine ($An_{48}Ab_{51}Or_1$), labradorite ($An_{64}Ab_{35}Or_1$), and potassic feldspar ($An_0Ab_2Or_{98}$) were observed in one of the samples. Labradorite is probably the primary plagioclase phase in the basalts, whereas andesine may represent partially albitized precursor plagioclase. The pyroxenes are diopside, based on the Morimoto *et al.* (1988) classification, which is consistent with pyroxene compositions from the Sarmiento Complex (cf., Calderón *et al.*, 2007b). The metamorphic minerals are albite, amphibole, chlorite, epidote, titanite, occasional garnet, and trace amounts of K-feldspar. The amphiboles are actinolite and magnesiohornblende.

The chlorite that was analyzed belongs to the clinochlore–chamosite series and has a tetrahedral Si content of 5.4 to 6.3 per formula unit, based on a base of O = 28. Small amounts of Ca, Na, and K could be due to the presence of tiny inclusions of other minerals. The compositions of the chlorites from metabasalts of the Rocas Verdes ophiolites (including those from the Sarmiento Complex; Calderón, 2006) were compared in an XFe vs. Si diagram (Fig. 3) with chlorites from the present sea floor (Laverne *et al.*, 1995), the Horokanai ophiolite (Ishizuka, 1985), and Archean rocks taken by Kitajima *et al.* (2001), and these all show a comparable dispersion pattern.

Epidote in the three analyzed samples contains 9.7 to 16.5 wt% Fe_2O_3, and XFe^{3+} is between 0.21 and 0.38.

Tortuga Complex

The Tortuga ophiolite is exposed in an east–west-trending 20-km-wide belt extending from the southwestern part of the Isla Navarino (Fig. 1) to the region south of the Canal Beagle. The southern border of the ophiolite

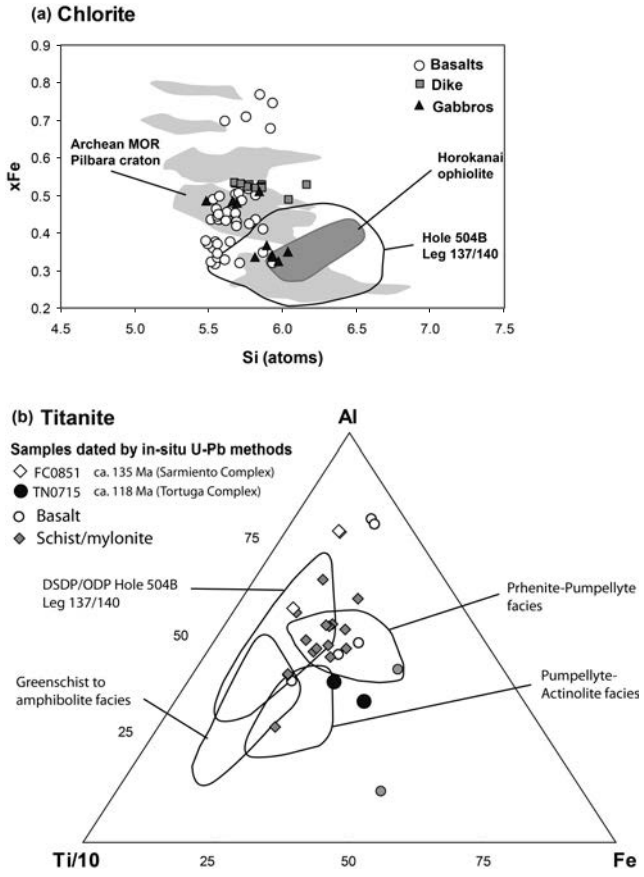

Fig. 3. (a) Chemical compositions of chlorite plotted on an XFe vs. SiO_2 Hey diagram (Hey, 1954) for chlorites of the Rocas Verdes ophiolites and from different related environments: DSDP Hole 504B (Alt et al., 1982; Laverne et al., 1995) and the Horokanai ophiolite (Ishizuka, 1985); and (b) Al–Fe–Ti/10 diagram for titanite of the Sarmiento and Tortuga complexes compared with that from other metamorphic facies/environments.

is in fault contact with a tightly folded and weakly foliated package of turbiditic rocks. To the north, the possible depositional contact between the Tortuga ophiolite and sedimentary rocks is obscured by subsequent thrust-fold deformation and earliest Late Cretaceous plutons (Hervé *et al*., 1984). The Tortuga ophiolite is remarkable for its exceptional exposures of mafic oceanic-like crustal pseudostratigraphy, which grades upward from cumulate gabbros to pillow and sheet-flow basalts (Godoy, 1978; Stern, 1979). The extrusive unit of the Tortuga ophiolite consists of a more than 2000-m-thick succession of submarine volcanic rocks, including massive and pillowed basalts, volcanic breccias, hyaloclastites, and intercalated horizons of chert and siltstones. The basalts bear plagioclase and clinopyroxene, and some contain subordinate pseudomorphs after discernible primary orthopyroxene and olivine. Pillow basalts preserve a fine-grained variolitic texture, with skeletal plagioclase laths and fans of dendritic clinopyroxene. Massive lava flows, or diabase sills, with characteristic columnar structures have medium-grained ophitic and variolitic textures of plagioclase intergrown with pyroxene granules. Massive diabase screens within a 1-km-thick level of sheeted dikes consist of medium-grained plagioclase and clinopyroxene and orthopyroxene and have ophitic, subophitic, intergranular, and poikilitic textures. The exposed base of the Tortuga ophiolite consists of an igneous complex made up of slightly altered massive and layered gabbros, most of which are two pyroxene and olivine gabbros, leucogabbros, and clinopyroxene troctolites intruded by dikes of basalt and fine diabase with chilled margins.

In the uppermost extrusive levels of the ophiolite, Godoy (1978) described the coexistence of chlorite, pumpellyite, albite, and carbonate in amygdales and pumpellyite, prehnite, quartz, and zeolites in veins. The igneous mineral assemblage of the examined samples is replaced to varying degrees (30–90%) by combinations of chlorite, titanite, epidote, carbonate, actinolite, and rare hornblende. Plagioclase is albitized and is replaced by epidote, titanite, and subordinate chlorite, actinolite, and/or white mica. Clinopyroxene displays narrow rims of epidote, actinolite, titanite, and localized chlorite. Orthopyroxene and olivine are pseudomorphed by chlorite. Serpentine and traces of titanite and carbonate also occur as a result of olivine alteration. The primary interstitial groundmass has been recrystallized to chlorite, titanite, epidote, and carbonate. Various generations of veins are filled mostly by chlorite in combination with titanite, prehnite, quartz, epidote, hornblende, actinolite, biotite, and carbonate. Amygdales consist of combinations of chlorite, epidote, plagioclase, actinolite, hornblende, quartz, titanite, prehnite, and opaque minerals. A summary of the secondary minerals is shown in Fig. 2.

In the diabase bodies, metamorphism has affected approximately 40 to 80% of the rocks and the mineral assemblages consist of albite, chlorite, titanite, actinolite, hornblende, epidote, quartz, traces of white mica, and leucoxene. Plagioclase is albitized and partially replaced by epidote and chlorite and subordinate titanite, actinolite, and white mica. The same secondary phases, together with quartz and subordinate titanite, occur in the groundmass or in interstices between primary igneous phases. Pyroxene is replaced by chlorite and actinolite. These rocks are intruded by fine diabase and aphanitic basaltic dikes, having similar alteration products, and are affected locally by brittle faults. Widespread narrow veins consist of prehnite with quartz, epidote, and chlorite. Opaque minerals are widespread.

In the gabbros, metamorphic phases are restricted to microstructures, such as microveins and fine crystal co-

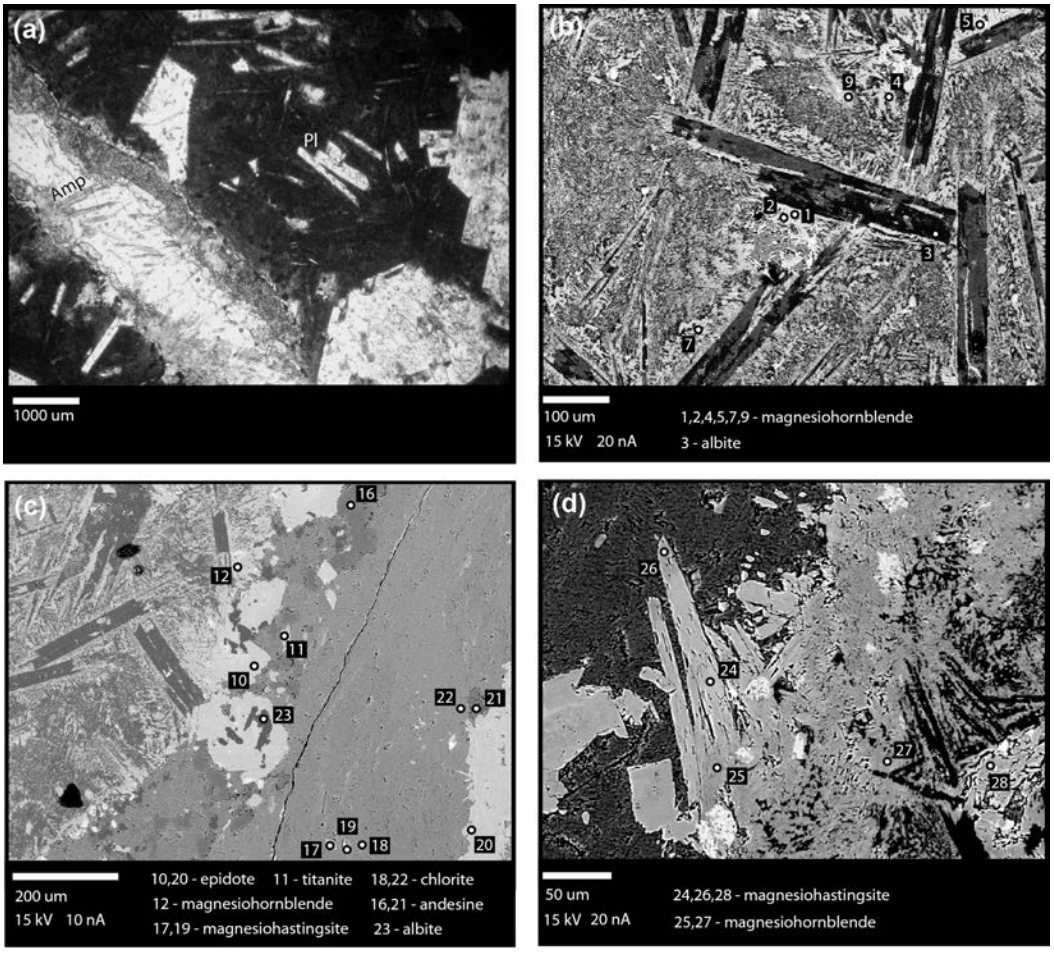

Fig. 4. (a) A photomicrograph and (b), (c), (d) back-scattered electron images of pillow basalt (sample TN0715) mostly replaced by secondary metamorphic minerals but retaining its original igneous texture. Abbreviations are Amp, amphibole; Pl, plagioclase.

ronae. Epidote, clinozoisite, and titanite are the most common secondary phases in plagioclase, which is also replaced by varying amounts of white mica and actinolite. Pyroxenes host patches that include actinolite, chlorite, epidote, and rare aggregates of titanite; however, pyroxenes are replaced by biotite and white mica in weakly banded gabbroic hornfelses. Olivine commonly hosts microfractures filled with clay aggregates (iddingsite) and occasionally serpentine, talc, and subordinate actinolite and titanite. Microveins consist of varying amounts of chlorite, epidote, clinozoisite, serpentine and rare white mica, actinolite, and pumpellyite. Rare and restricted amphibolites and biotite-bearing hornfelsic rocks occur adjacent to basaltic dikes, evidencing processes of contact metamorphism. Although the widespread metamorphic overprint in the ophiolite is essentially non-deformational, centimeter-thick bands of brecciated gabbroic rocks with veins of epidote, chlorite, prehnite, tremolite, and calcite are also present.

Mineral chemistry Secondary minerals from sample TN0715 were analyzed. A selection of the mineral analyses is given in Table S1, and textural relationships are illustrated in Fig. 4.

Phenocrysts of plagioclase are pure albite. Plagioclase in the rims of veins has a composition of andesine or albite. The amphiboles in the groundmass and in veins correspond to magnesiohornblende and magnesiohastingsite.

METAMORPHISM

The mineral assemblages and textural relationships in the examined rocks vary, so it is difficult to determine accurate pressure-temperature metamorphic conditions. Hence, we discuss metamorphic grade constraints using phase relations calculated for typical mid-ocean ridge basalts, which according to Massonne and Willner (2008) indicate that (1) prehnite occurs at pressures <4 kbar and at temperatures <250°C; (2) epidote is stable at temperatures >200°C; (3) pumpellyite is stable at temperatures

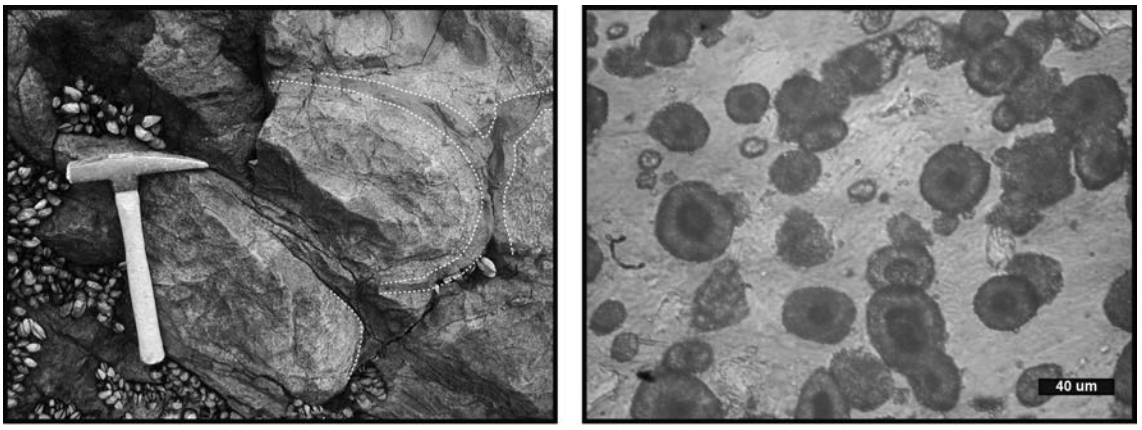

Fig. 5. (a) Pillow basalts from the Tortuga ophiolite with aphanitic "devitrified" margins from which sample TN0715 was collected; and (b) a microscopic image of the spherical microaggregates of titanite (sample TN0715A2) from the Tortuga Complex considered to represent fossil bacteria.

<300°C; (4) biotite crystallization begins at temperatures of about 320°C; (5) titanite disappears at temperatures >550°C; and (6) chlorite is stable at temperatures up to about 600°C. It is worth mentioning that pressure conditions of approximately 2 kbar during non-deformative burial metamorphism can be explained by the overlying turbiditic succession of the Yaghan Formation that reaches thickness of more than 3000 m (Katz, 1964) and as much as 6000 m in some areas (Winn and Dott, 1978); the Formation has concordant diabase sills and basalt intercalations. Higher-pressure conditions could have existed in foliated metabasalts, which have mineral assemblages indicative of greenschist-facies dynamic metamorphism related to obduction and deformation of ophiolitic complexes.

Mineral assemblages in undeformed rocks of the Capitán Aracena and Carlos III complexes are indicative of prehnite–pumpellyite facies metamorphism, in which the coexistence of epidote, prehnite, and pumpellyite permit estimation of temperatures of metamorphism between 200 and 250°C. Another group of undeformed rocks has mineral assemblages that include albite, actinolite, biotite, chlorite, epidote, clinozoisite, quartz, titanite, rare garnet, and hornblende, which is indicative of greenschist-facies metamorphic conditions with intermediate temperature conditions of between 350 and 500°C.

In the highly recrystallized extrusive and diabase dike levels of the Tortuga Complex, chlorite, epidote, titanite, and actinolite are ubiquitous phases and biotite, white mica, and hornblende occur in minor amounts. A well-examined sample from this complex (TN0715A) contains Mg-rich hornblende and hastingsite, biotite, titanite, chlorite, epidote, andesine, and albite, which are distinctive of the greenschist facies and/or the greenschist–amphibolite metamorphic facies transition (temperatures between 320 and 550°C). Conversely, the gabbroic level is less recrystallized and hosts minor amounts of titanite, epidote, actinolite, hornblende, biotite, and clinozoisite. Late prehnite-bearing veins in the diabase dike and gabbroic levels are associated with retrograde products that crystallized at temperatures below 250°C.

Local variations of the mineral assemblages in undeformed rocks could reflect particular pressure-temperature conditions of formation and/or changes in fluid composition during prograde and/or retrograde metamorphism (e.g., sample TN0715A). The presence of epidote, titanite, and amphibole suggests the involvement of Ca–Al rich metamorphic fluids. These elements and K, required for the crystallization of biotite (in veins and pyroxene) and white mica (in plagioclase), were probably leached from intermediate-to-calcic plagioclase of igneous origin or derived from metasomatism during the emplacement of mafic ophiolitic magmas (or, in the case of K, later granitoid plutons). Conversely, in the least-recrystallized gabbroic level, we suggest that the cooling of gabbroic rocks and the associated heat release produced a thermal barrier that prevented circulation of percolating fluids close to the lowermost ophiolitic portions where crystallization occurred proximal to the spreading axis. This suggestion is in agreement with previous observations (cf., Stern *et al*., 1976; Godoy, 1978)

BIOALTERATION OF BASALTS

Biogenetic microstructures are common features in glassy volcanic rocks recovered from the upper portion of the oceanic crust at more than thirty localities in the major oceans and a few marginal basins and have been documented in several ophiolites and greenstone belts (see GSA Data Repository Table DR1, 2006). Microbiotic al-

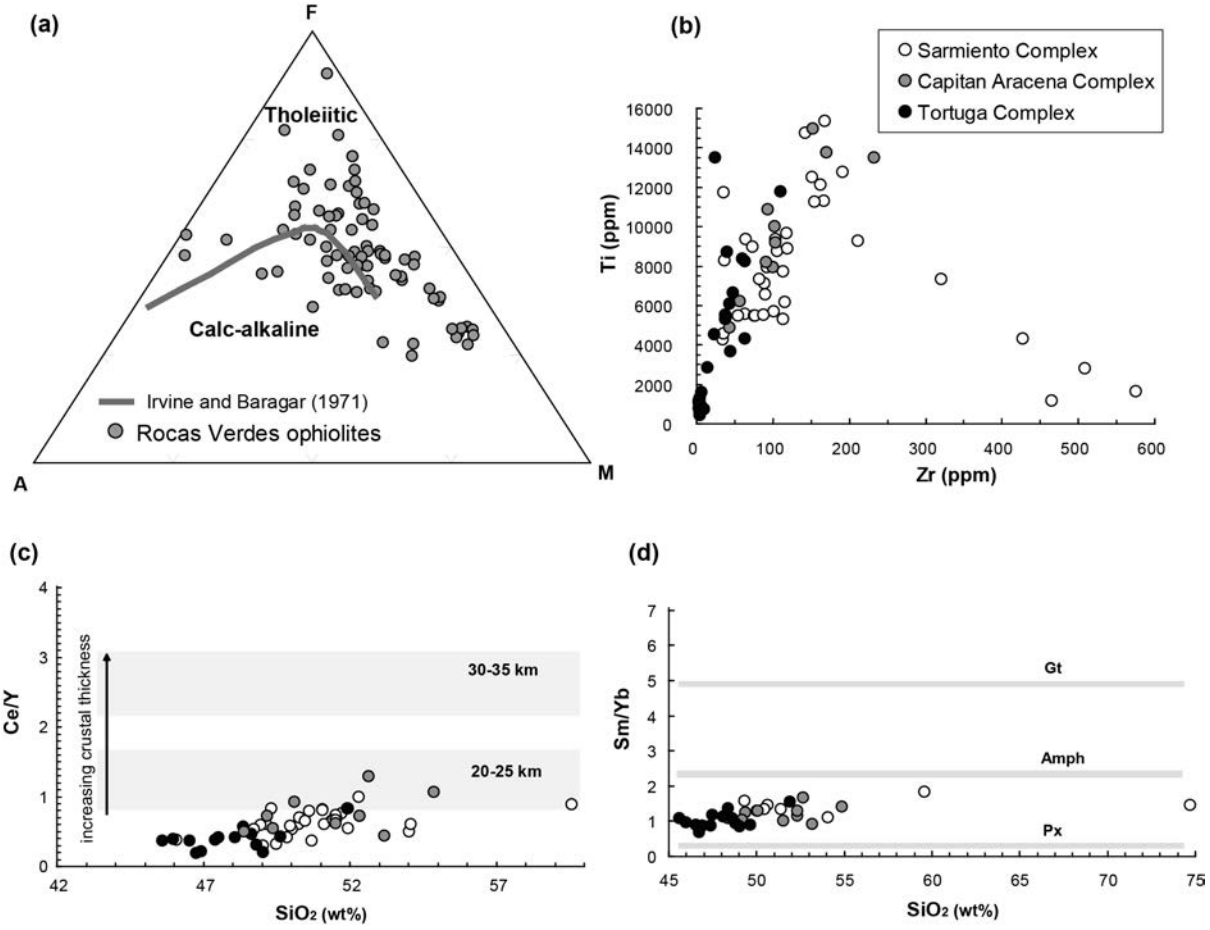

Fig. 6. Geochemical and petrological features of pillow basalts, basaltic dikes, diabases, and gabbroic rocks of the different ophiolite complexes as shown in (a) AFM, (b) Ti vs. Zr, (c) Ce/Y, and (d) Sm/Yb vs. SiO_2 diagrams. In (c) the crustal thickness associated with the Ce/Y ratios in basaltic rocks is indicated (cf., Mantle and Collins, 2008). In (d) Sm/Yb ratios are related to residual mineralogy in equilibrium with magmas (cf., Kay and Kay, 1991). Abbreviations are Px, pyroxene; Amph, amphibole; Gt, garnet. Geochemical data are from Stern (1979, 1980), Saunders et al. (1979), Fildani and Hessler (2005), and this study.

teration is generally documented at the edges of fractured glass in pillow basalts, where circulation of seawater promotes microbial growth (Staudigel *et al*., 2006). According to Furnes and Staudigel (1999), bioalteration can be traced to depths of nearly 550 m in the oceanic crust but predominates at depths of about 300 m.

Spherical and concentric aggregates of titanite (Fig. 5b) and rare tubular microstructures found in veins within the chilled margin of pillowed metabasalts (Fig. 5a; sample TN0715A) have sizes and shapes that are comparable to those of microorganisms found in modern oceanic crust and structures in other ophiolites. The spherical polycrystalline bodies consist mainly of cryptocrystalline (0.5 μm) titanite and subordinate silicate and opaque phases, as determined by EMP analysis, back-scattered electron images, selected-area electron diffraction analysis, and transmission electron microscopy images (Avendaño, 2008). The mineral chemistry of the titanite is shown in an Al–Fe–Ti/10 diagram (Fig. 3), in which the compositions of the titanite are compared with those from different environments. The bodies may record processes of microbial colonization at temperatures and depths compatible with the existence of life. Microbial tests may be preserved by aggregates of microcrystalline titanite that crystallized during the greenschist- to amphibolite-facies metamorphic overprinting.

GEOCHEMISTRY

Geochemical data from mafic rocks of the Rocas Verdes ophiolites provide constraints on compositional features of the mantle source of mafic magmas derived during rift to back-arc basin evolution. Existing data are combined here with new major, trace, and rare earth element (REE) bulk-rock compositions from the Capitán Aracena, Carlos III, and Tortuga complexes (Table S2).

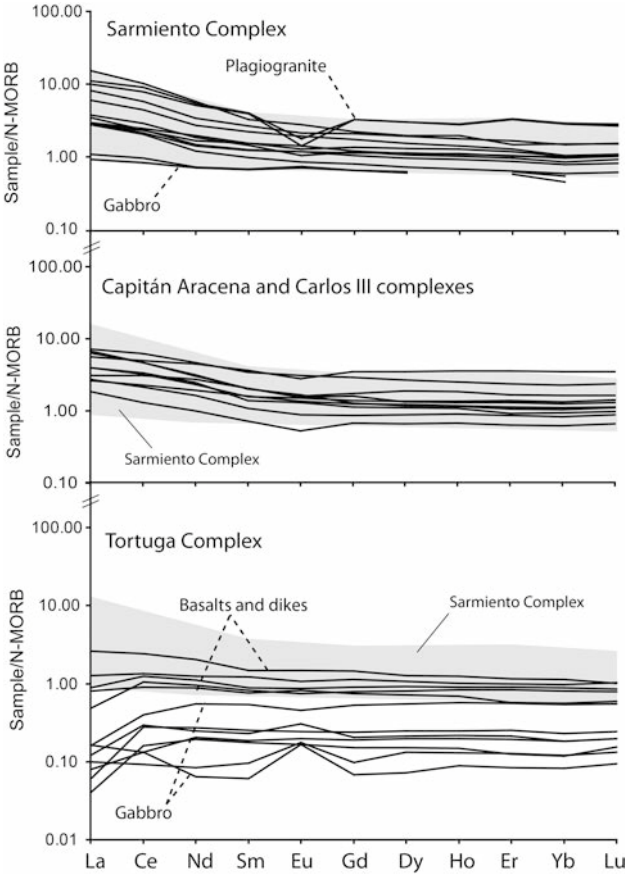

Fig. 7. Normal mid-ocean ridge basalt (N-MORB) normalized rare earth element diagram of the ophiolite complexes of the Rocas Verdes basin, using the normalization values of Sun and McDonough (1989). Geochemical data are from Stern (1979), Saunders et al. (1979), Fildani and Hessler (2005), and this study.

One common feature among these is that the metabasalts have a high degree of alteration that is reflected in the loss on ignition (LOI), some varying from *ca*. 3–5%. All samples, including lavas, dikes, and gabbros, show a tholeiitic differentiation trend (Fig. 6a) in the AFM diagram of Irvine and Baragar (1971), which is confirmed by other diagrams shown below.

Capitán Aracena and Carlos III complexes

Seven samples from Isla Capitán Aracena and three from Isla Carlos III were analyzed. Six samples from Capitán Aracena complex are basalts and one correspond to a basaltic andesite; two samples from Carlos III complex are basalts and one is a basaltic andesite.

Ti abundances are very useful for distinguishing tholeiitic and calc–alkaline basalts because these reflect crystallization processes that occur during magmatic evolution (Miyashiro, 1973; Pearce, 1982). Tholeiitic magmas are characterized by increasing Ti contents during the early stages of differentiation (reflecting the fractionation of olivine and pyroxene ± plagioclase) followed by decreasing contents in the later stages because of fractionation of magnetite (cf., Miller *et al*., 1994). In contrast, Ti abundances of calc–alkaline magmas decrease consistently during differentiation due to early fractionation of Fe–Ti oxides with olivine and clinopyroxene (±plagioclase) (Sisson and Grove, 1993). Figure 6b shows Ti vs. Zr abundances of samples from the Capitán Aracena Complex, which define trends characteristic of tholeiitic magmas. A similar differentiation pattern was noted for published data for the Rocas Verdes ophiolites (Stern, 1979, 1980). The Ce/Y vs. SiO_2 diagram (cf., Mantle and Collins, 2008) is compatible with the concept of a thinned crust resulting from extension in a rift or back-arc environment (Fig. 6c), and the Sm/Yb vs. SiO_2 plot suggests differentiation that was controlled by clinopyroxene (Fig. 6d).

REE diagrams normalized to the composition of normal mid-oceanic ridge basalts (Fig. 7) show a great similarity between the Sarmiento and Capitán Aracena complexes; these are more enriched in large-ion lithophile elements than is the Tortuga Complex, which suggests that the former have a greater affinity with enriched mid-oceanic ridge basalts. Basaltic rocks of both localities in the Capitán Aracena Complex have relatively flat REE patterns; however, those of the Carlos III Complex are steep and more enriched in light REEs and hence display enriched mid-oceanic ridge basalt affinities.

Tortuga Complex

The Tortuga ophiolite, the southernmost ophiolitic remnant of the Rocas Verdes basin, has been considered to record the most advanced evolutionary stage of the basin opening to a mid-ocean ridge-type setting (cf., Saunders *et al*., 1979; Stern, 1979). Mafic rocks crystallized from tholeiitic basaltic magmas with mid-oceanic ridge basalt geochemical affinities (Stern, 1979; Avendaño, 2008) probably generated by decompression melting of the sub-back-arc mantle. These relationships are well shown by the diagrams of Fig. 7, in which rocks from the Tortuga and Capitán Aracena complexes are compared with rocks from the Sarmiento Complex.

U–Pb GEOGHRONOLOGY

The Rocas Verdes ophiolites are considered to have formed during the Late Jurassic, based on U–Pb zircon crystallization ages for plagiogranites of the Sarmiento Complex in the southern Patagonian Andes (Calderón *et al*., 2007a) and from the Larsen Harbor ophiolitic complex of the island of South Georgia (Mukasa and Dalziel, 1996).

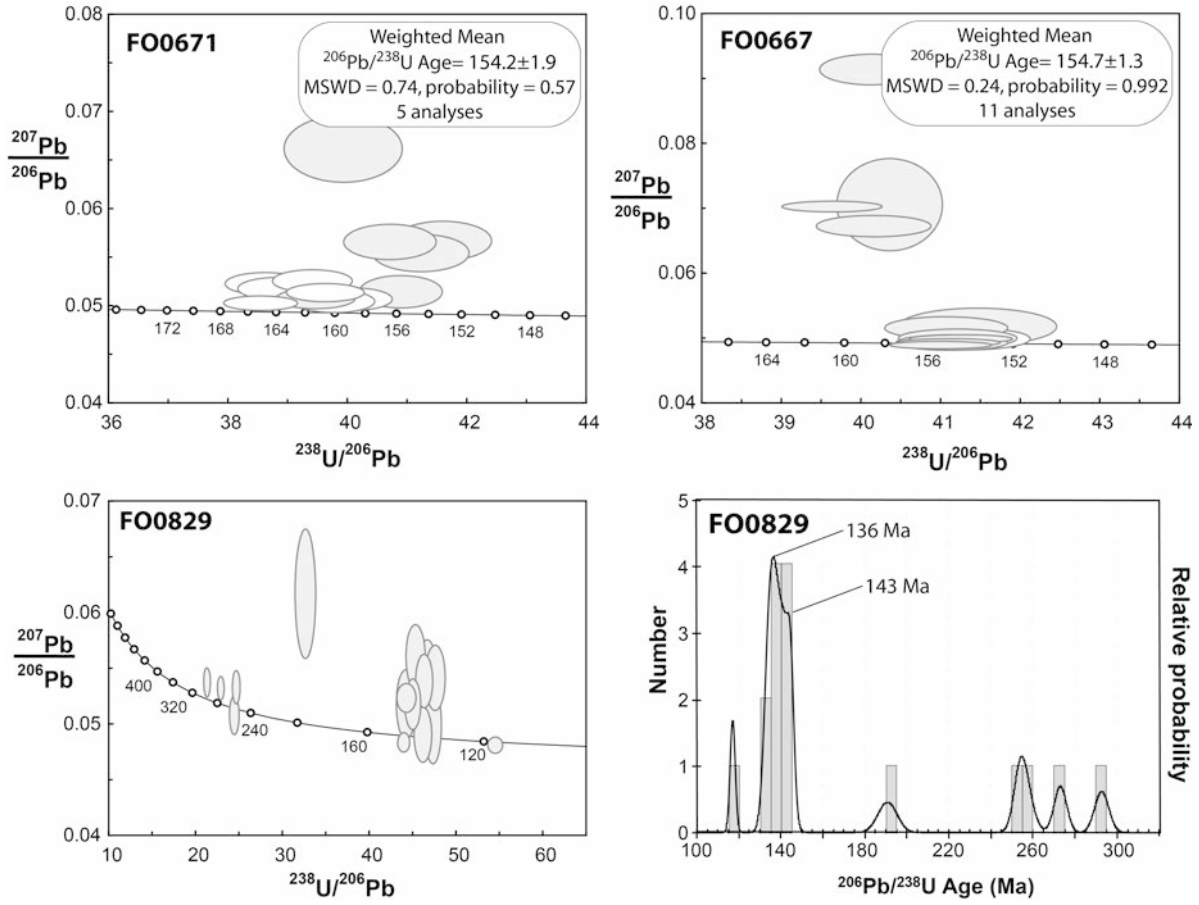

Fig. 8. Tera-Wasserburg diagrams for zircon samples dated during this work with the sensitive high-resolution ion microprobe (SHRIMP). Grey ellipses indicate the analyses considered for the calculation of the weighted mean age. The age vs. probability diagram for sample FO0829 (for ages below 300 Ma) is also shown.

Calderón *et al*. (2007a) reported additional zircon crystallization ages relevant to the timing of bimodal magmatic activity associated with the generation of the Sarmiento Complex. These indicate ages of 149.1 ± 1.5 Ma for a plagiogranite intruded into gabbros and 151.0 ± 1.5 Ma for a dacite dike crosscutting pillow basalts. These ages are older and more precise than the results of 147 ± 10 Ma for a trondjhemite and 139 ± 2 Ma for a plagiogranite dike reported by Stern *et al*. (1992). Calderón *et al*. (2012) reported U–Pb data for zircons and $^{40}Ar/^{39}Ar$ data for amphiboles from plutons and lamprophyric dikes, respectively, that cut deformed rocks of the Sarmiento Complex. These undeformed intrusives yielded crystallization ages of about 80 Ma, thus placing constraints on the time of deformation of the ophiolites. A similar zircon crystallization age of 80 Ma was reported for a coarse-grained granite that intrudes the basaltic rocks at Puerto Tilly, Isla Carlos III but also shows strong inheritance of 150 Ma zircons (Hervé *et al*., 2007a).

U–Pb zircon ages

There has been a lack of geochronological data for the mafic rocks from the Capitán Aracena and Tortuga complexes; however, three new SHRIMP U–Pb ages from zircon are presented in this paper (Table S3).

One of the samples is a medium-grained gabbro from Seno Elisa (FO0671), which was collected 100 m below pillow basalts having no discontinuity with the underlying rocks (Fig. 8). This gabbro yielded a weighted mean age of 154.2 ± 1.9 Ma, which is the oldest age obtained for ophiolitic rocks from the Rocas Verdes ophiolites. The other igneous sample is from a vaguely foliated coarse-grained leucogranite (FO0667; Fig. 8), which is intruded by foliated mafic dikes at the northwestern end of Fjord Dyneley. This sample yielded a weighted mean age of 154.7 ± 1.3 Ma. These ages indicate that the early rifting stage of Rocas Verdes basin development was accompanied by bimodal magmatism south of the Magallanes–Fagnano transform fault, a major tectonic boundary since the pre-Jurassic (Hervé *et al*., 2010).

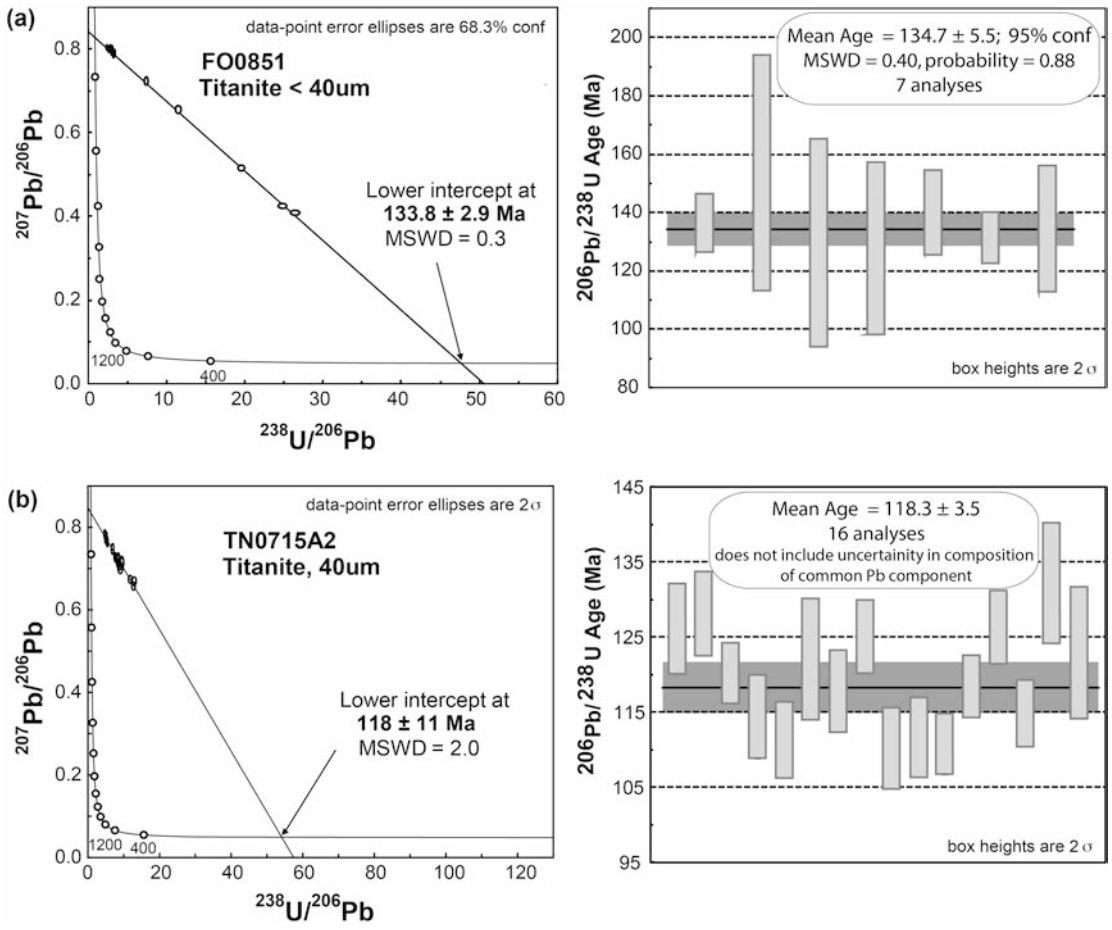

Fig. 9. Tera-Wasserburg diagrams and U–Pb weighted mean ages for titanite grains from (a), (b) felsic phyllonite (FC0851) from the Canal de las Montañas shear zone and (c), (d) metabasalt from the Tortuga Complex (TN0715A2), using the SHRIMP and LA-MC-ICP-MS, respectively. The horizontal black line and dark gray band in (b) and (d) show the inferred age and uncertainty of the syngenetic titanite.

A cherty layer directly overlying pillow basalts on the east coast of Isla Thomson (sample FO0829) yielded two dominant groups of zircon ages, about 136 and 143 Ma (Fig. 8). Other detrital zircons from the rock have Permian, Cambrian, latest Neoproterozoic, and Grenvillian ages. This outcrop at Isla Thomson is an outlier of the main body of the Tortuga ophiolitic complex.

U–Pb titanite ages

Titanite from pre-tectonic relics in phyllonites (FC0851) of the basal, low-grade metamorphic sole of the Sarmiento Complex yielded a SHRIMP U–Pb mean crystallization age of roughly 135 Ma (Figs. 9a and b; Table S4a). The high uncertainty is due to the high contents of common Pb in titanite. On the basis of textural relationships and chemical composition (Fig. 3), this result probably represents the age of seafloor-like metamorphism in a back-arc setting.

Sixteen spherical aggregates of titanite (microbe-like structures; sample TN0715A) with a mean diameter of 40 μm were dated by U–Pb LA-MC-ICP-MS (Table S4b). The in situ analyses yielded a latest Early Cretaceous mean crystallization age of 118.3 ± 3.5 Ma (Figs. 9c and d). The uncertainties of the ages propagate and include all sources of error (at the 2 sigma level; cf., Simonetti *et al.*, 2006). Because the titanite is in association with amphibole, epidote, chlorite, plagioclase, and quartz in veins within the outer zone or margins of pillow basalts, this age constrains an Aptian episode of high-temperature greenschist facies metamorphism.

DISCUSSION

Seafloor metamorphism in a suprasubduction setting

Mineral assemblages and textural relationships in the studied rocks indicate prevalent fluid-assisted, low-to-intermediate temperature, non-deformational metamor-

phism throughout the extrusive and diabase levels of the ophiolitic complexes, which were progressively covered by thick successions of hemipelagic sediments and volcanoclastic turbidites. It has been documented that volcanic rocks in mid-ocean ridge settings are less rapidly covered by sedimentary successions and so are commonly altered to low-temperature zeolite facies assemblages (Alt, 1999; Shibuya *et al*., 2007). In contrast, the predominance of prehnite–pumpellyite and higher temperature greenschist facies parageneses documented in volcanic rocks from suprasubduction ophiolites (Gillis and Banerjee, 2000) are thought to be related to rapid burial under thick sedimentary successions. Thus, the early tectono/metamorphic evolution of the Rocas Verdes ophiolites, before basin closure and intrusion of earliest Late Cretaceous plutonic rocks, can be attributed to seafloor hydrothermal metamorphism in a suprasubduction setting.

Aptian upper age limit for mafic back-arc magmatism

Stratigraphic and sedimentological constraints from the Rocas Verdes basin (Katz, 1964; Watters, 1965; Suárez and Pettigrew, 1976; Winn and Dott, 1978; Suárez *et al*., 1985; Fildani and Hessler, 2005) indicate that ophiolitic crust was progressively covered by successions of hemipelagic sediments and volcanoclastic turbidites derived from the erosion of a proximal active (or remnant) volcanic arc and pre-Jurassic continental basement rocks having zircon detrital components of Permian, Cambrian, and latest Neoproterozoic ages (cf., Calderón *et al*., 2007a). The absence of precise geochronological data in the mafic rocks and a precise biostratigraphic record in the sedimentary rocks make it difficult to establish an upper age limit of mafic back-arc magmatism. This topic is discussed below.

As a first approximation, the detrital zircon ages from the cherty layer intercalated within the pillow basalts at Isla Thomson (an outlier of the Tortuga Complex) suggest a maximum of Valanginian or younger age of back-arc mafic magmatism. This is consistent with detrital zircon ages reported for fine-grained turbidites from the Zapata and Yaghan formations (Calderón *et al*., 2007a; Hervé *et al*., 2010), indicating maximum depositional ages of Hauterivian for the sedimentary successions and a 25 myr minimum time period of continuous sedimentation in the Rocas Verdes basin.

Additional evidence is provided by the U–Pb age, roughly 118 Ma, for the concentric spheroids of titanite related to an Aptian episode of high-temperature greenschist-facies hydrothermal metamorphism. It is conceivable that magmatism and intermediate-temperature alteration were contemporaneous with high thermal gradients associated with major extension of the back-arc lithosphere. The latter is also suggested by geochemical

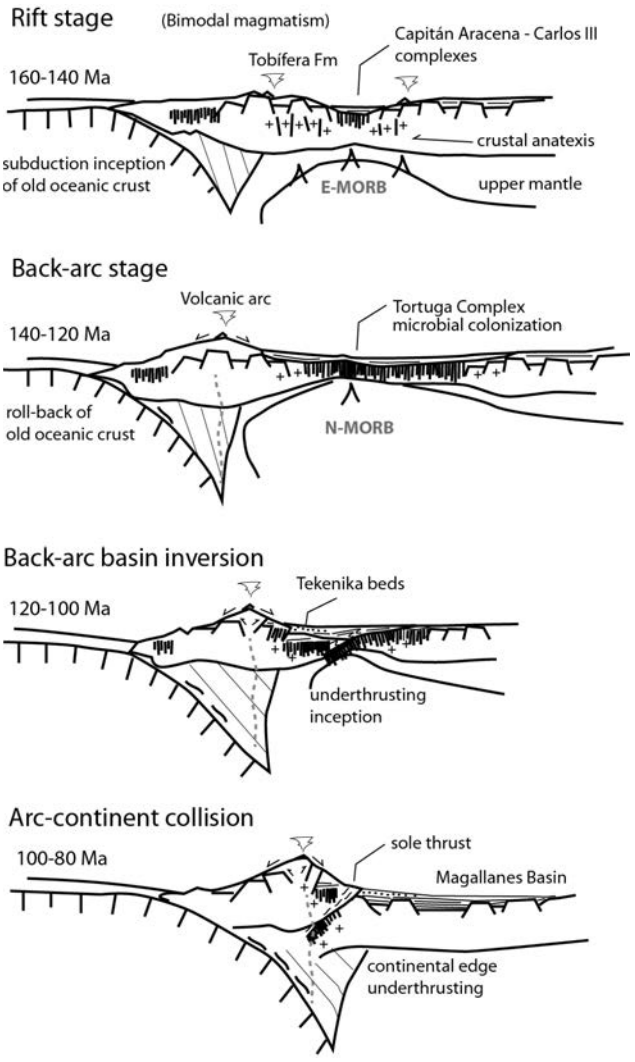

Fig. 10. Schematic reconstructions of the environment of deposition of the Rocas Verdes basin based on data presented in this work and previous studies (Cunningham, 1994; Hervé and Fanning, 2003; Stern and de Wit, 2003; Fildani and Hessler, 2005; Calderón et al., 2007a, 2007b, 2007c, 2012; Klepeis et al., 2010; Maloney et al., 2011).

data from the ophiolitic rocks (Fig. 6c). Although titanite precipitation could have occurred immediately or up to 20 my after the bioalteration processes, as noted in other ophiolitic complexes (Furnes *et al*., 2001), on the basis of mineralogical and textural evidence from metabasalts of the Tortuga Complex, it is thought that the titanite was probably precipitated soon after the mafic magmatism near the spreading/magmatic axis. This scenario supports the possibility that the oceanic-like crust of the Rocas Verdes basin was generated within a period of about 35 myr, during which the latest back-arc basin stage probably overlapped with the onset of the Aptian–Albian An-

dean orogeny in Tierra del Fuego (Dott *et al*., 1977) signaled by the deposition of the conglomerates of the Tekenika Beds. Thus, during the early phase of basin closure, which was probably related to changes in subduction parameters along a continental margin on the Pacific side and opening of the Atlantic Ocean, waning mafic back-arc magmatism was followed by underthrusting of the Rocas Verdes basin seafloor beneath the drifted magmatic arc.

Tectonic emplacement of the ophiolites

In ophiolitic complexes in which rocks are foliated and metamorphosed in a discontinuous way, the overprint of deformation events is probably associated with thrust-fold deformation and shearing and strike-slip faulting during basin closure (cf., Cunningham, 1993; Klepeis *et al*., 2010). The petrological study of the Canal de las Montañas shear zone and the identification of the metamorphic sole of the Sarmiento Complex (Calderón *et al*., 2012) both provide insights into the tectonic processes related to the closure of quasi-oceanic basins developed at convergent margins. The tectonic emplacement of the Sarmiento Complex resulted in different generations of shear zones and folds associated with several thrust-deformation events. In particular, a continent-ward reverse sense of shearing and thermobarometric constraints of *ca*. 5–6 kbar and 230–260°C for mylonites indicate that the primary shearing event was related to a west-dipping underthrusting in a subduction zone setting (Hervé *et al*., 2007b; Calderón *et al*., 2012). Although the inception age of underthrusting or subduction within the Rocas Verdes basin is a matter for further study, combined zircon U–Pb and phengite $^{40}Ar/^{39}Ar$ age data reveal that the main ophiolitic obduction phase and juxtaposition of the Sarmiento Complex and its metamorphic sole occurred before 80 Ma. Similar crystallization ages of about 80 Ma obtained from granites crosscutting ophiolite complexes at Carlos III and the Gordon and Navarino islands suggest a regional tectono-magmatic event. Paleogeographic reconstructions based on our data (Fig. 10) and the interpretations summarized above indicate the generalized evolution of the Rocas Verdes basin and a possible fate of ophiolitic complexes developed in a suprasubduction setting.

Conclusions

The Rocas Verdes ophiolites represent a Late Mesozoic analogue for Archean greenstone belts and present-day marginal basins developed at convergent margins. The tectonic evolution of ophiolitic complexes in southern Chile entails an interplay between processes of seafloor, burial, shearing, and contact metamorphism during the evolution of the Late Mesozoic Rocas Verdes basin. Late Jurassic (*ca*. 154 Ma) ophiolite generation was coeval with abundant siliceous magmatism inside, or in the surroundings of, the nascent ophiolite in an extensional environment related to the break-up of Gondwana. Bimodal magmatism during the initial rift stage was followed by tholeiitic mafic magmatism, comparable to mid-oceanic ridge basalts, in the back-arc region. This mafic magmatism was active until the earliest Cretaceous (*ca*. 118 Ma). New geochronological data indicate that submarine mafic magmatism within the Rocas Verdes basin persisted for at least *ca*. 35 myr in mid-oceanic ridge-type spreading systems that were sites of microbial colonization of seafloor hydrothermal environments. The tectonic emplacement of the ophiolite bodies involved the underthrusting of the continental edge of South America beneath the drifted arc sliver and was completed before the latest Cretaceous (*ca*. 80 Ma), as indicated by crystallization ages of crosscutting granitoids.

Acknowledgments—This is a contribution to Project Anillo Antártico ACT-105 of CONICYT-PBCYT and to the BMBF-CONICYT program linked to the FONDECYT 1095099 project. Colleagues Marcelo Solari, Bob Pankhurst, Edgardo Dzogolyk, Leonardo Fadel Cury, Esteban Salazar, Manuel Suárez, Augusto Rapalini and Stuart Thomson participated during different fieldwork campaigns. Captains Gilles Rigaud and Sebastian Magnen onboard the *Morgane*, Conrado Alvarez onboard the *Penguin*, and Hugo Cárdenas onboard the yacht *Chonos* provided a safe trip to these remote areas. We thank Professor Luis Aguirre for fruitful conversations and discussions about low-grade metamorphism and continuous support during the development of the graduation theses of two of the co-authors. Drs. Yuji Orihashi and Ryo Anma provided encouragement that helped us prepare this contribution. We acknowledge Charles R. Stern and Andrea Fildani for their constructive and thoughtful reviews.

References

Alabaster, T. and Storey, B. C. (1990) Modified Gulf of California model for South Georgia, north Scotia Ridge, and implications for the Rocas Verdes back-arc basin, southern Andes. *Geology* **18**, 497–500.

Allen, R. B. (1982) Geología de la Cordillera Sarmiento, Andes Patagónicos, entre los 51°00′ y 52°15′ Lat. S, Magallanes, Chile. *Servicio Nacional de Geología y Minería*, *Boletín* **38**, 1–46.

Alt, J. C. (1999) Very low-grade hydrothermal metamorphism of basic igneous rocks. *Low-Grade Metamorphism* (Frey, M. and Robinson, D., eds.), 169–201, Blackwell Science Ltd.

Alt, J. C., Laverne, C. and Muehlenbachs, K. (1982) Alteration of the upper oceanic crust: mineralogy and processes in Deep Sea Drilling Project Hole 504B, Leg 83. *Initial Reports of the Deep Sea Drilling Project* **83**, 217–247.

Anonymous (1972) Penrose field conference on ophiolites. *Geotimes* **17**, 24–25.

Avendaño, V. (2008) Petrología del Complejo Ofiolítico

Tortuga, Magallanes Chile: Evidencias de un metamorfismo Cretácico Inferior. Graduate Thesis, Univ. Chile, 128 pp.

Bruhn, R. L., Stern, C. R. and de Wit, M. J. (1978) Field and geochemical data bearing on the development of a Mesozoic volcano-tectonic rift zone and back-arc basin in southernmost South America. *Earth Planet. Sci. Lett.* **41**, 32–46.

Calderón, M. (2006) Petrogenesis and tectonic evolution of Late Jurassic bimodal magmatic suites (Sarmiento Complex) and migmatites (Puerto Eden Igneous and Metamorphic Complex) in the southern Patagonian Andes. Ph.D. Thesis, Univ. Chile, 174 pp.

Calderón, M., Fildani, A., Hervé, F., Fanning, C. M., Weislogel, A. and Cordani, U. (2007a) Late Jurassic bimodal magmatism in the northern seafloor remnant of the Rocas Verdes basin, southern Patagonian Andes. *J. Geol. Soc. London* **164**, 1011–1022.

Calderón, M., Hervé, F., Cordani, U. and Massonne, H.-J. (2007b) Crust-mantle interactions and the generation of silicic melts: insights from the Sarmiento Complex, southern Patagonian Andes. *Rev. Geol. Chile* **34**, 249–275.

Calderón, M., Hervé, F., Massonne, H.-J., Tassinari, C. G., Pankhurst, R. J., Godoy, E. and Theye, T. (2007c) Petrogenesis of the Puerto Eden igneous and metamorphic complex, Magallanes, Chile: Late Jurassic anatexis of metagreywackes and granitoid magma genesis. *Lithos* **93**, 17–38.

Calderón, M., Fosdick, J. C., Warren, C., Massonne, H.-J., Fanning, C. M., Fadel Cury, L., Schwanethal, J., Fonseca, P. E., Galaz, G., Gaytán, D. and Hervé, F. (2012) The low-grade Canal de las Montañas shear zone and its role on the tectonic emplacement of the Sarmiento ophiolitic complex and Late Cretaceous Patagonian Andes orogeny, Chile. *Tectonophysics* **524–525**, 165–185.

Cunningham, W. D. (1993) Strike-Slip faults in the southernmost Andes and the development of the Patagonian Orocline. *Tectonics* **12**, 169–186.

Cunningham, W. D. (1994) Uplifted ophiolitic rocks on Isla Gordon, southernmost Chile: implications for the closure history of the Rocas Verdes marginal basin and the tectonic evolution of the Beagle Channel region. *J. S. Am. Earth Sci.* **7**, 135–147.

Dalziel, I. W. D. (1981) Back-arc extension in the southern Andes: a review and critical reappraisal. *Phil. Trans. R. Soc. A* **300**, 319–335.

Dalziel, I. W. D. (1986) Collision and Cordilleran orogenesis. *Collision Tectonics* (Coward, M. P. and Ries, A. C., eds.), *Geol. Soc. Spec.* **19**, 389–404, Geological Society of London.

Dalziel, I. W. D., de Wit, M. J. and Palmer, K. F. (1974) Fossil marginal basin in the southern Andes. *Nature* **250**, 291–294.

Dalziel, I. W. D., Lawver, L. A. and Murphy, J. B. (2000) Plumes, orogenesis, and supercontinental fragmentation. *Earth Planet. Sci. Lett.* **178**, 1–11.

Dilek, Y. (2003) Ophiolite pulses, mantle plumes and orogeny. *Ophiolites in Earth History* (Dilek, Y. and Robinson, P. T., eds.), *Geol. Soc. Spec. Publ.* **218**, 9–19, Geological Society of London.

Dilek, Y. and Furnes, H. (2011) Ophiolite genesis and global tectonics: Geochemical and tectonic fingerprinting of ancient oceanic lithosphere. *Geol. Soc. Am. Bull.* **123**, 387–411.

Dott, R. H., Winn, R. D., de Wit, M. J. and Bruhn, R. L. (1977) Tectonic and sedimentary significance of Cretaceous Tekenika Beds of Tierra del Fuego. *Nature* **266**, 620–622.

Elthon, D. and Stern, C. R. (1978) Metamorphic petrology of the Sarmiento ophiolite complex, Chile. *Geology* **6**, 464–468.

Fildani, A. and Hessler, A. M. (2005) Stratigraphic record across a retroarc basin inversion: Rocas Verdes–Magallanes basin, Patagonian Andes, Chile. *Geol. Soc. Am. Bull.* **117**, 1596–1614.

Fildani, A., Cope, T. D., Graham, S. A. and Wooden, J. L. (2003) Initiation of the Magallanes foreland basin: Timing of the southernmost Patagonian Andes orogeny revised by detrital zircon provenance analysis. *Geology* **31**, 1081–1084.

Fosdick, J., Romans, B., Fildani, A., Bernhardt, A., Calderón, M. and Graham, S. A. (2011) Kinematic evolution of the Patagonian retroarc fold-thrust belt and Magallanes foreland basin, Chile and Argentina, 51°30′ S. *Geol. Soc. Am. Bull.* **123**, 1679–1698.

Fuenzalida, R. and Covacevich, V. (1988) Volcanismo y bioestratigrafía del Jurásico y Cretácico Inferior en la Cordillera Patagónica, Región de Magallanes, Chile. *V Congreso Geológico Chileno* (Corvalán, J. and Charrier, R., eds.), H159–H183, Santiago, Chile.

Furnes, H. and Staudigel, H. (1999) Biological mediation in ocean crust alteration: how deep is the deep biosphere? *Earth Planet. Sci. Lett.* **166**, 97–103.

Furnes, H., Muehlenbachs, K., Tumyr, O., Torsvik, T. and Xenophontos, C. (2001) Biogenic alteration of volcanic glass from the Troodos ophiolite, Cyprus. *J. Geol. Soc. London* **158**, 75–84.

Furnes, H., Banerjee, N. R., Muehlenbachs, K., Staudigel, H. and de Wit, M. (2004) Early life recorded in Archean pillow lavas. *Science* **304**, 578–581.

Gillis, K. M. and Banerjee, N. R. (2000) Hydrothermal alteration patterns in suprasubduction zone ophiolites. *Ophiolites and Oceanic Crust: New Insights from Field Studies and the Ocean Drilling Program* (Dilek, Y., Moores, E. M., Elthon, D. and Nicolas, A., eds.), *Geol. Soc. Am. Spec. Paper* **349**, 283–297, Geological Society of America.

Godoy, E. (1978) Observaciones en el Complejo Ofiolítico de Isla Milne Edwards-Cerro Tortuga (Isla Navarino) Magallanes-Chile. VII Congreso Geológico Argentino, Neuquén, Actas, II, 625–636.

GSA Data Repository Table DR1 (2006) Available at ftp://rock.geosociety.org

Hervé, F. and Fanning, C. M. (2003) Early Cretaceous subduction of continental crust at the Diego de Almagro archipelago, southern Chile. *Episodes* **26**, 285–289.

Hervé, F., Pankhurst, R. J., Fanning, C. M., Calderón, M. and Yaxley, G. M. (2007a) The South Patagonian batholith: 150 my of granite magmatism on a plate margin. *Lithos* **97**, 373–394.

Hervé, F., Massonne, H.-J., Calderón, M. and Theye, T. (2007b) Metamorphic *P–T* conditions of Late Jurassic rhyolites in the Magallanes fold and thrust belt, Patagonian Andes,

Chile. *J. Iber. Geol*. **33**, 5–16.
Hervé, F., Fanning, C. M., Pankhurst, R. J., Mpodozis, C., Klepeis, K., Calderón, M. and Thomson, S. N. (2010) Detrital zircon SHRIMP U–Pb age study of the Cordillera Darwin Metamorphic Complex of Tierra del Fuego: sedimentary sources and implications for the evolution of the Pacific margin of Gondwana. *J. Geol. Soc. London* **167**, 555–568.
Hervé, M., Suárez, M. and Puig, A. (1984) The Patagonian batholith S of Tierra del Fuego, Chile: Timing and tectonic implications. *J. Geol. Soc. London* **141**, 909–917.
Hey, M. H. (1954) A new review of the chlorites. *Mineral. Mag*. **30**, 277–292.
Irvine, T. N. and Baragar, W. R. A. (1971) A guide to the chemical classification of the common volcanic rocks. *Can. J. Earth Sci*. **8**, 523–548.
Ishizuka, H. (1985) Prograde metamorphism of the Horokanai ophiolite in the Kamuikotan Zone, Hokkaido, Japan. *J. Petrol*. **26**, 391–417.
Katz, H. R. (1964) Some new concepts on geosynclinal development and mountain building at the southern end of South America. *Proc. 22nd International Geological Congress, India, New Delhi* **4**, 242–255.
Katz, H. R. and Watters, W. A. (1966) Geological investigation of the Yahgán Formation (upper Mesozoic) and associated igneous rocks of Navarino Island, southern Chile. *New Zeal. J. Geol. Geop*. **9**, 323–359.
Kay, R. W. and Kay, S. M. (1991) Creation and destruction of lower continental crust. *Geol. Rundsch*. **80**, 259–278.
Kitajima, K., Maruyama, S., Utsunomiya, S. and Liou, J. G. (2001) Sea-floor hydrothermal alteration at an Archaean mid-ocean ridge. *J. Metamorph. Geol*. **19**, 583–599.
Klepeis, K., Betka, P., Clarke, G., Fanning, M., Hervé, F., Rojas, L., Mpodozis, C. and Thomson, S. N. (2010) Continental underthrusting and obduction during the Cretaceous closure of the Rocas Verdes rift basin, Cordillera Darwin, Patagonian Andes. *Tectonics* **29**, TC3014, doi:10.1029/2009TC002610.
Laverne, C., Vanko, D. A., Tartarotti, P. and Alt, J. C. (1995) Chemistry and geothermometry of secondary minerals from the deep sheeted dike complex, Hole 504B. *Proc. ODP, Sci. Results*, **137/140**, 167–189.
Leake, B. E., Woolley, A. R., Arps, C. E. S., Birch, W. D., Gilbert, M. C., Grice, J. D., Hawthorne, C., Kato, A., Kisch, H. J., Krivovichev, V. G., Linthout, K., Laird, J., Mandarino, J. A., Maresch, W. V., Nickel, E. H., Rock, N. M. S., Schumacher, J. C., Smith, D. C., Stephenson, C. N., Ungaretti, L., Whittaker, E. J. W. and Youzhi, G. (1997) Nomenclature of amphiboles: report of the subcommittee on amphiboles of the International Mineralogical Association, Commission on new minerals and mineral names. *Am. Mineral*. **82**, 1019–1037.
Ludwig, K. R. (2000) SQUID 1.00, A User's Manual, Berkeley Geochronology Center Special Publication, n. 2, 2455 Ridge road, Berkeley, CA 94709, U.S.A.
Maloney, K. T., Clarke, G. L., Klepeis, K. A., Fanning, C. M. and Wang, W. (2011) Crustal growth during back-arc closure: Cretaceous exhumation history of Cordillera Darwin, southern Patagonia. *J. Metamorph. Geol*. **29**, 649–672.
Mantle, G. W. and Collins, W. J. (2008) Quantifying crustal thickness variations in evolving orogens: correlation between arc basalt composition and Moho depth. *Geology* **36**, 87–90.
Massonne, H.-J. and Willner, A. (2008) Dehydration behaviour of metapelites and mid-ocean ridge basalt at very-low to low grade metamorphic conditions. *Eur. J. Mineral*. **20**, 867–879.
Miller, C. A., Barton, M., Hanson, R. and Flemming, T. (1994) An Early Cretaceous volcanic arc-marginal basin transition zone, Peninsula Hardy, southernmost Chile. *J. Volcanol. Geoth. Res*. **63**, 33–58.
Miyashiro, A. (1973) The Trodos ophiolitic complex was probably formed in an island-arc. *Earth Planet. Sci. Lett*. **19**, 218–224.
Morimoto, N., Fabries, J., Ferguson, A. K., Ginzburg, I. V., Ross, M., Seifert, F. A., Zussman, J., Aoki, K. and Gottardi, G. (1988) Nomenclature of pyroxenes. *Am. Mineral*. **73**, 1123–1133.
Mukasa, S. B. and Dalziel, I. W. D. (1996) Southernmost Andes and South Georgia island, north Scotia Ridge: zircon U–Pb and muscovite Ar/Ar age constraints on tectonic evolution of southwestern Gondwanaland. *J. S. Am. Earth Sci*. **9**, 349–365.
Otzen, G. (1987) Geología Regional de la isla Capitán Aracena y Clarence, Magallanes, Chile. Informe Técnico ENAP (in edit report).
Pankhurst, R. J., Riley, T. R., Fanning, C. M. and Kelley, S. P. (2000) Episodic silicic volcanism in Patagonia and the Antarctic Peninsula: Chronology of magmatism associated with the break-up of Gondwana. *J. Petrol*. **41**, 603–625.
Pearce, J. (1982) Trace element characteristics of lavas from destructive plate boundaries. Andesites: *Orogenic Andesites and Related Rocks* (Thorpe, R. S., ed.), 525–548, Wiley, New York.
Pearce, J. A., Lippard, S. J. and Roberts, S. (1984) Characteristics and tectonic significance of suprasubduction zone ophiolites. *Marginal Basin Geology: Volcanic and Associated Sedimentary and Tectonic Processes in Modern and Ancient Marginal Basins* (Kokelaar, B. P. and Howells, M. F., eds.), *Geol. Soc. Spec. Publ*. **16**, 77–96, Geological Society of London.
Prades, C. F. (2008) Petrología y metamorfismo de las rocas basálticas en la isla Capitán Aracena, isla Carlos III y Estero La Pera, Region de Magallanes, Chile. Graduate Thesis, Univ. Chile, 135 pp.
Rapalini, A. E., Calderón, M., Singer, S., Hervé, F. and Cordani, U. (2008) Tectonic implications of a paleomagnetic study of the Sarmiento Ophiolitic Complex, southern Chile. *Tectonophysics* **452**, 29–41.
Romans, B. W., Fildani, A., Graham, S. A., Hubbard, S. M. and Covault, J. A. (2010) Importance of predecessor basin history on sedimentary fill of a retroarc foreland basin: provenance analysis of the Cretaceous Magallanes basin, Chile (50°52′ S). *Basin Res*. **22**, 640–658.
Saunders, A. D., Tarney, J., Stern, C. R. and Dalziel, I. W. D. (1979) Geochemistry of Mesozoic marginal basin floor igneous rocks from southern Chile. *Geol. Soc. Am. Bull*. **90**, 237–258.

Shibuya, T., Komiya, T., Anma, R., Ota, T. and Omori, S. (2007) Progressive metamorphism of the Taitao ophiolite; evidence for axial and off-axis hydrothermal alterations. *Lithos* **98**, 233–260.

Simonetti, A., Heaman, L. M., Chacko, T. and Banerjee, N. R. (2006) *In situ* thin section U–Pb dating of zircon, monazite, and titanite using laser ablation-MC-ICP-MS. *Int. J. Mass Spectrom*. **253**, 87–97.

Sisson, T. and Grove, T. (1993) Experimental investigations of the role of H_2O in calc–alkaline differentiation and subduction zone magmatism. *Contrib. Mineral. Petrol*. **113**, 143–166.

Staudigel, H., Furnes, H., Banerjee, N. R., Dilek, Y. and Muehlenbachs, K. (2006) Microbes and volcanoes: A tale from the oceans, ophiolites, and greenstone belts. *GSA Today*, **16**, 4–10.

Stern, C. R. (1979) Open and closed system igneous fractionation within two Chilean ophiolites and the tectonic implications. *Contrib. Mineral. Petrol*. **68**, 243–258.

Stern, C. R. (1980) Geochemistry of Chilean ophiolites: evidence for the compositional evolution of the mantle source of back-arc basin basalts. *J. Geophy. Res*. **85**, 955–966.

Stern, C. R. (1991) Isotopic composition of Late Jurassic and Early Cretaceous mafic igneous rocks from the southernmost Andes: implications for sub-Andean mantle. *Rev. Geol. Chile* **18**, 15–23.

Stern, C. R. and de Wit, M. J. (2003) Rocas Verdes ophiolites, southernmost South America: remnants of progressive stages of development on oceanic-type crust in a continental margin back-arc basin. *Ophiolites in Earth History* (Dilek, Y. and Robinson, P. T., eds.), *Geol. Soc. Spec. Publ.* **218**, 1–19, Geological Society of London.

Stern, C. R., de Wit, M. J. and Lawrence, J. R. (1976) Igneous and metamorphic processes associated with formation of Chilean ophiolites and their implications for ocean floor metamorphism, seismic layering, and magnetism. *J. Geophy. Res*. **81**, 4370–4380.

Stern, C. R., Mukasa, S. and Fuenzalida, R. (1992) Age and origin of silicic rocks in the Sarmiento complex of the Rocas Verdes ophiolites, southernmost Chile. *J. S. Am. Earth Sci*. **6**, 32–40.

Stetter, K. O. (2006) Hyperthermophiles in the history of life. *Phil. Trans. R. Soc. B* **361**, 1837–1843.

Suárez, M. and Pettigrew, T. H. (1976) An upper Mesozoic island-arc-back-arc system in the southern Andes and South Georgia. *Geol. Mag*. **113**, 305–328.

Suárez, M., Hervé, M. and Puig, A. (1985) Hoja Isla Hoste e islas adyacentes: XII Región, escala, 1:250.000. IIG, Carta Geológica de Chile (65), Santiago, 106 pp.

Sun, S. and McDonough, W. (1989) Chemical and isotopic systematics of oceanic basalts: implications for mantle composition and processes. *Magmatism in Ocean Basins* (Saunders, A. and Norry, M., eds.), *Geol. Soc. Spec. Publ.* **42**, 313–345, Geological Society of London.

Tera, F. and Wasserburg, G. (1972) U–Th–Pb systematics in three Apollo 14 basalts and the problem of initial Pb in lunar rocks. *Earth Planet. Sci. Lett*. **14**, 281–304.

Thorseth, I. H., Torsvik, T., Torsvik, V., Daae, F. L., Pedersen, R. B. and Keldysh-98 Scientific Party (2001) Diversity of life in ocean floor basalts. *Earth Planet. Sci. Lett*. **194**, 31–37.

Vaughan, A. P. M. and Scarrow, J. H. (2003) Ophiolite obduction pulses as a proxy indicator of superplume events? *Earth Planet. Sci. Lett*. **213**, 407–416.

Watters, W. A. (1965) Prehnitization in the Yahgan formation of Navarino island, southernmost Chile. *Mineral. Mag*. **268**, 517–527.

Williams, I. S. (1998) U–Th–Pb geochronology by ion microprobe. *Applications of Microanalytical Techniques to Understanding Mineralizing Processes* (McKibben, M. A., Shanks, W. C., III and Ridley, W. I., eds.), *Rev. Eco. Geol*. **107**, 1–35, Society of Economic Geologists.

Wilson, T. J. (1991) Transition from back-arc to foreland basin development in southernmost Andes: stratigraphic record from the Ultima Esperanza District, Chile. *Geol. Soc. Am. Bull*. **103**, 98–111.

Winn, R. D. and Dott, R. H. (1978) Submarine-fan turbidites and resedimented conglomerates in a Mesozoic arc-rear marginal basin in southern South America. *Sedimentation in Submarine Canyons, Fans, and Trenches* (Stanley, D. J. *et al*., eds.), 362–372, Hutchison & Ross, Inc., Dowden.

SUPPLEMENTARY MATERIALS

URL (http://www.terrapub.co.jp/journals/GJ/archives/data/47/MS235.pdf)
Tables S1 to S4